
FOR THE RECORD

Lipid-binding proteins: Structure of the phospholipid ligands

DEREK MARSH

Max-Planck-Institut für biophysikalische Chemie, 37070 Göttingen, Germany

(RECEIVED March 21, 2003; FINAL REVISION May 22, 2003; ACCEPTED May 22, 2003)

Abstract

Dihedral angles are evaluated for the phospholipid ligands of the lipid-binding proteins found in the Protein Data Base (PDB). Phospholipid structures occur with a *trans* C1–C2 configuration of the glycerol backbone and oppositely extended chains, in addition to the *gauche* C1–C2 rotamers found in membranes. Headgroup conformations are not restricted to the single bent-down configuration and *gauche–gauche* configuration of the phosphodiester that is found in phospholipid crystals. Additionally, fully extended headgroups and orientations directed away from the lipid chains are found for phospholipids in the protein binding pockets. On average, the hydrocarbon chains of the protein-bound lipids are conformationally more disordered than in fluid bilayer membranes. However, much of this configurational disorder arises from energetically disallowed *skew* conformations. This suggests a configurational heterogeneity in the lipids at a single binding site: Eclipsed conformations occur also in some lipid headgroups and glycerol backbones. Stereochemical violations appear for some of the ester carboxyl groups of the protein-bound phospholipids in the PDB, and two glycerol backbones have the incorrect enantiomeric configuration.

Keywords: Lipase; phospholipase; phospholipid transfer protein; saposin; permeability-increasing protein; ultraspiracle protein

Phospholipid-binding proteins are an important component of cellular signalling, trafficking, and metabolism (for a review, see Hurley et al. 2000). The conformations of the phospholipid ligands bound to these various proteins, and their relation to those of phospholipids in the bilayer membrane pool, are therefore of considerable interest. Crystal structures are now available for phospholipids bound to several proteins of the above classes (see Table 1). For phospholipid transfer proteins (Yoder et al. 2001; Roderick et al. 2002) the natural substrate, and for phospholipase A₂ inhibitor phospholipids (Scott and Sigler 1994), have been resolved in the X-ray structure. Phospholipids have also been identified bound to lipases (van Tilbeurgh et al. 1993; Brzozowski et al. 2000), to saposin B (Ahn et al. 2003), to catechol-1,2-dioxygenase (Vetting and Ohlendorf 2000), to a flavohaemoprotein (Ollesch et al. 1999), to the endothelial

protein C receptor (Oganessian et al. 2002), and (as a heterologous ligand) to an orphan nuclear receptor (Billas et al. 2001).

The purpose of the present communication is to classify the various phospholipid structures associated with the different phospholipid-binding protein classes, by evaluating dihedral angles. A significant consideration is the extent to which these correspond to energetically allowable rotamers. High-energy single conformers can be an indicator for the presence of conformational heterogeneity. With saposin B, evidence was found for additional conformers, in both the headgroup and acyl chains of the partially ordered phosphatidylethanolamine molecule (Ahn et al. 2003).

Figure 1 shows LIGPLOT (Wallace et al. 1995) schematic diagrams of different phospholipid ligands associated with various lipid-binding proteins. It is evident that the relative arrangement of the two lipid chains and the orientation of the lipid headgroup vary greatly, depending on the configuration of the protein binding pocket. The chains may be parallel (Fig. 1A,C), splayed (Fig. 1B), or even bent back around the headgroup (Fig. 1D). The headgroup may be

Reprint requests to: Derek Marsh, Max-Planck-Institut für biophysikalische Chemie, Abt. Spektroskopie, 37070 Göttingen, Germany; e-mail: dmarsh@gwdg.de; fax: 49-551-201-1501.

Article and publication are at <http://www.proteinscience.org/cgi/doi/10.1110/ps.0396803>.

Table 1. Source of coordinates for phospholipids in crystals of soluble proteins

PDB name	Lipid/protein ^a	PDB file	Res. (Å) ^b	References
PC2 501	Ole ₂ PtdCho/ratPI-TP α	1FVZ	2.20	Yoder et al. 2001
PC2 577,578	Ste ₂ PtdCho/human bpip	1EWF	1.70	Kleiger et al. 2000
PLC 601,701,801	Lau ₂ PtdCho/ <i>Th. lanuginosa</i> lipase	1EIN	3.00	Brzozowski et al. 2000
PLC 1	Lau ₂ PtdCho/human pancreatic lipase	1LPA	3.04	van Tilbeurgh et al. 1993
DPL 2313	Lin ₂ PtdCho/human PC-TP	1LN1	2.40	Roderick et al. 2002
CPL 300,301	Pal-linPtdCho/human PC-TP	1LN3	2.90	Roderick et al. 2002
LIO 999,1999	Pentadec-decPtd(Cho)/Ac 1,2-CTD	1DMH	1.70	Vetting and Ohlendorf 2000
PEH 300	Ste ₂ PtdEtn/human saposin B	1N69	2.20	Ahn et al. 2003
EPH 4000	Ste-palPtdEtn/ <i>H. virescens</i> USP	1G2N	1.65	Billas et al. 2001
PTY 606,607	Pentadec-achPtdEtn/human rsEPCR	1LQV	1.60	Oganesyan et al. 2002
DGG 406(A),(B)	Pal-(cp)palPtd(Etn/Gro)/ <i>A. eutrophus</i> FHP	1CQX	1.75	Ollesch et al. 1999

^a Ste, stearoyl; ole, oleoyl; lau, lauroyl; lin, linoleoyl; pal, palmitoyl; pentadec, pentadecanoyl; dec, decanoyl; ach, arachidoyl; (cp)pal, *cis*-9,10-methylene-palmitoyl; PtdCho, phosphatidylcholine; PtdEtn, phosphatidylethanolamine; PtdGro, phosphatidylglycerol; PI-TP, phosphatidylinositol transfer protein; bpip, bactericidal permeability-increasing protein; PC-TP, phosphatidylcholine transfer protein; Ac 1,2-CTD, catechol-1,2-dioxygenase/*Acinetobacter* sp. ADP1; USP, ultraspiracle protein; rsEPCR, recombinant soluble endothelial protein C receptor; FHP, flavohaemoprotein.

^b Resolution of structure determination.

bent back (Fig. 1B), extended (Fig. 1C), displaced relative to the chains (Fig. 1A), or strongly coiled (Fig. 1D). Analysis and classification is possible from the dihedral angles for the phospholipid backbone and headgroup.

Table 2 lists the headgroup (α_1 – α_5), glycerol backbone (θ_1 – θ_4), and acyl chain (γ_1 . . . , β_1 . . .) torsion angles for diacyl phosphatidylcholine or phosphatidylethanolamine bound to the proteins listed in Table 1. Corresponding torsion angles for phospholipid inhibitors of phospholipase A₂ (PLA₂) are listed in Table 3. Of the inhibitors, GEL is a phospholipid transition-state analog with a heptylphosphonyl *sn*-2 chain, and both INB and DHG have amide-blocked *sn*-2 chains. These latter phospholipids are bound to different classes of secretory and pancreatic phospholipases A₂. For comparison, the torsion angles of phosphatidylcholine (Pearson and Pascher 1979), and phosphatidylethanolamine (Elder et al. 1977) in lamellar single crystals are also included in Table 2. The notation used for defining the phospholipid torsion angles is that given by Pascher et al. (1992; see Fig. 2). The C-atoms of the glycerol backbone are numbered according to the *sn*-system. Those of the headgroup are designated C $_{\alpha}$ and C $_{\beta}$, outwards from the phosphate.

Some estimate of the reliability of the torsion angles can be obtained by comparing the data for CPL 300 and CPL 301, which correspond to the two molecules in the asymmetric unit for the human PC-TP. The largest difference between the two sets of torsion angles in Table 2 is 21°, and the mean absolute difference is 7° ($N = 17$). Extending the data sets up to β_{14} and γ_{11} , the maximum difference remains in the region 20–30°, with a mean absolute difference of 10° ($N = 34$). Deviations become larger, however, towards the ends of the hydrocarbon chains. Six of the remaining β_n and γ_n torsion angles have deviations of approximately 60°, corresponding to the difference between adjacent staggered and eclipsed conformers. For one further C–C bond, the

torsion angle (γ_{14}) actually reverses sign between CPL 300 and CPL 301. These large deviations indicate an increasing segmental disorder towards the ends of the phospholipid acyl chains, even in the crystal. For the two PTY molecules in the asymmetric unit of EPCR crystals, all torsion angles in Table 2, with the exception of γ_3 and γ_4 , are well within 20° of one another, and the mean absolute deviation is 10° ($N = 17$). For the two equivalent LIO molecules bound to the 1,2-CTD homodimer, all torsion angles in Table 2, with the exception of β_4 , are within 25° of one another, and the mean absolute deviation is again 10° ($N = 17$). For the two DGG molecules in the asymmetric unit of FHP crystals, much larger differences are found between equivalent torsion angles in Table 2. As will be seen later, this arises because one of the two structures is the incorrect glycerol enantiomer. The data for the INB 201–206 inhibitors in Table 3 correspond to the six molecules of synovial PLA₂ per asymmetric unit. Thus, each molecule corresponds to only 17% of the total diffracting matter (Oh 1995). Nevertheless, with one exception, the standard deviations of torsion angles for the glycerol backbone and lipid chains in Table 3 are within approximately 30°. This is true also for the headgroup torsion angles α_1 and α_2 , but beyond this the headgroup is apparently disordered, as is the *sn*-1 chain from γ_7 onwards.

Glycerol backbone configuration

Table 4 summarizes configurational data on the glycerol backbone for the bound lipids in Tables 2 and 3. The difference between the complementary torsion angles θ_1 and θ_2 about the C2–C3 bond, and θ_3 and θ_4 about the C1–C2 bond, specifies the enantiomeric configuration. For the glycerol *sn*-3 phosphatidyl configuration, and tetrahedral carbon bonds, one expects that θ_1 – $\theta_2 = -120^\circ$ and

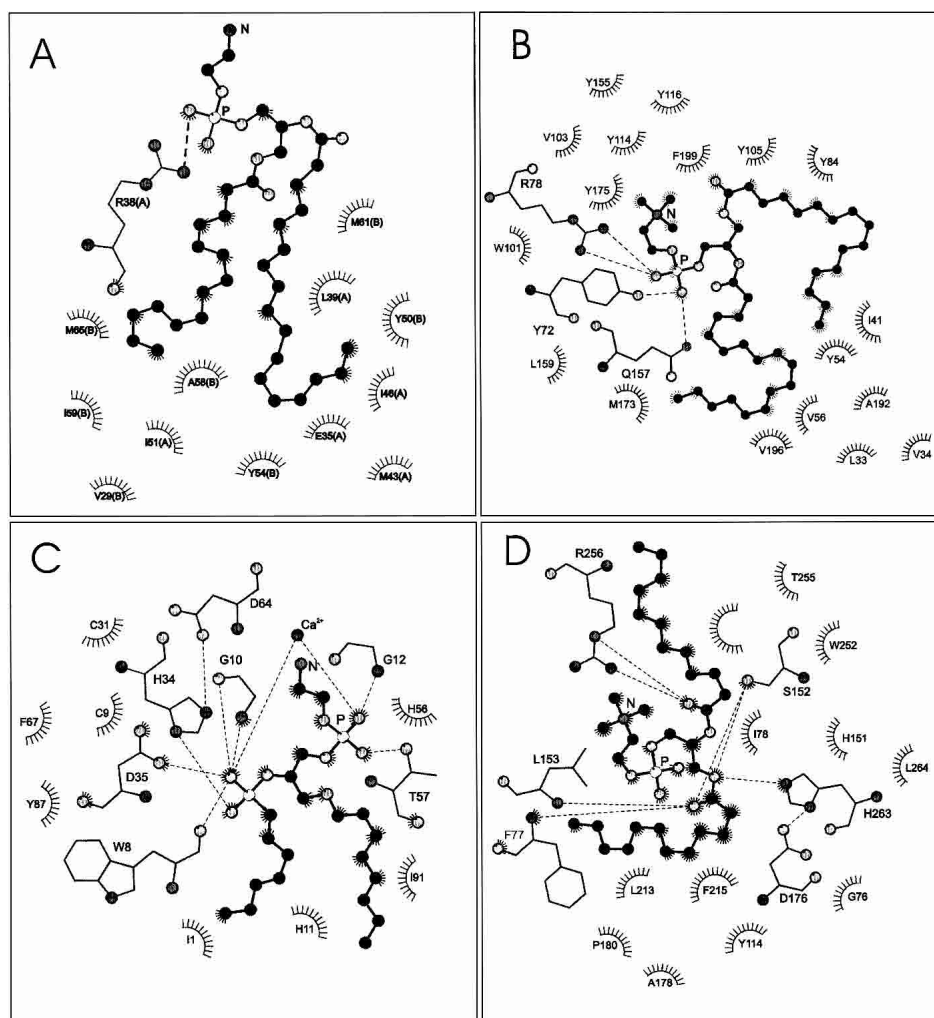


Figure 1. LIGPLOT diagrams (Wallace et al. 1995) of phospholipids associated with various lipid-binding proteins. Neighboring protein residues that are involved in hydrophobic contacts are indicated, and hydrogen bonds are shown explicitly. C-atoms of the phospholipid are shown as black balls. O-atoms are given in light gray, N-atoms in dark gray, and P-atoms are white. (A) Distearoyl phosphatidylethanolamine (PEH 300) bound to human saposin B (PDB:1N69; Ahn et al. 2003). (B) 1-Palmitoyl-2-linoleoyl phosphatidylcholine (CPL 301) bound to human phosphatidylcholine transfer protein (PDB:1LN3; Roderick et al. 2002). (C) 1-O-octyl-2-heptylphosphonyl-*sn*-glycero-3-phosphoethanolamine (GEL 420) bound to bee venom phospholipase A₂ (PDB:1POC; Scott et al. 1990). (D) Dilauroyl phosphatidylcholine (PLC 1) bound to human pancreatic lipase-procolipase complex (PDB:1LPA; van Tilbeurgh et al. 1993).

$\theta_3 - \theta_4 = +120^\circ$. This is found to be the case for all lipids except GEL 150 associated with pancreatic phospholipase A₂, PC2 501 associated with the phosphatidylinositol transfer protein (PI-TP), and DGG 406(B) associated with *Alcaligenes eutrophus* flavohaemoprotein (FHP). The latter two lipids possess definitively the incorrect (i.e., *sn*-1 phosphatidyl) glycerol stereoisomer.

The relative orientation of the two acyl chains is specified by the torsion angle θ_4 , and that of the headgroup relative to the chains by the torsion angle θ_2 (see Fig. 2). Following Pascher et al. (1992), the θ_4/θ_2 configuration is specified in terms of *sp* (*cis*), $\pm sc$ (*gauche*[±]), $\pm ac$ (*skew*[±]), or *ap* (*trans*) conformers with dihedral angles $0^\circ \pm 30^\circ$, $60^\circ \pm 30^\circ$,

$120^\circ \pm 30^\circ$, and $180^\circ \pm 30^\circ$, respectively. The configuration of the glycerol itself is specified by the θ_3/θ_1 combination of torsion angles. This complementary configuration is also given in Table 4, in terms of the more familiar *trans* (t), *gauche* (g), *skew* (s), and *cis* (c) conformers.

Almost all phospholipids associated with the secretory and pancreatic phospholipases A₂ have the $\theta_4/\theta_2 = sc/ap$ configuration. This corresponds to staggered glycerol rotamers, and allows approximately parallel alignment of the *sn*-1 and *sn*-2 chains (see Fig. 1C). The sole exceptions are INB 203, 205, and INB 201, associated with synovial PLA₂, the glycerol backbones of which contain one or two eclipsed rotamers, respectively. The *sc/ap* configuration is found

Table 2. Torsion angles ($^{\circ}$) of diacyl phosphatidylcholines (PC2, PLC, DLP, CPL, LIO) and phosphatidylethanolamine (PEH, EPH, PTY) in protein crystals, and of dimyristoyl phosphatidylcholine (DMPC) and dilauroyl phosphatidylethanolamine (DLPE) alone in lamellar crystals^a

Lipid ^b	α_1	α_2	α_3	α_4	α_5	θ_1	θ_2	θ_3	θ_4	β_1	β_2	β_3	β_4	γ_1	γ_2	γ_3	γ_4
DMPC A	163	62	68	143	-64	58	177	-178	63	82	172	-81	45	-177	168	-173	178
DMPC B	177	-74	-47	-150	54	168	-80	166	51	120	179	-134	67	102	176	170	180
DLPE	-154	58	66	106	67	-52	65	-172	69	97	179	-119	65	-178	173	179	-171
PC2 501	175	-35	-120	-167	143	-45	-154	-31	81	-139	-173	120	108	179	137	-30	-88
PC2 577	-159	167	37	-179	-27	139	-85	-80	148	-69	-4	-162	121	-161	-3	-158	-72
PC2 578								-96	143	104	92	111	-144	-145	114	-68	-59
PLC 601	178	-134	168	150	129	-113	20	168	38	56	-158	-81	-175	127	11	100	-134
PLC 701	-172	147	143	-128	-167	-50	76	172	46	50	-165	-109	129	159	8	-152	-139
PLC 801	-174	162	107	-168	-137	-57	68	169	41	47	-165	-113	150	148	15	-177	-140
PLC 1	157	88	131	-128	75	-58	72	-83	147	32	-64	-159	145	146	-82	-101	-116
DLP 2313	-148	176	15	177	178	144	-84	179	48	78	176	95	-97	-144	179	-50	128
CPL 300	-144	-177	19	-180	174	132	-99	180	54	74	178	105	-97	-111	177	-112	112
CPL 301	-152	-176	12	178	-176	139	-95	-177	56	87	178	87	-88	-122	175	-91	110
LIO 999	-141	(-66	179	84	180) ^c	137	-92	0	-129	-178	1	112	114	177	0	-150	180
LIO 1999	-166	(-59	180	79	180) ^c	129	-100	0	-130	180	1	124	167	177	0	-174	161
PEH 300	177	0	-172	-137	119	133	-105	159	24	61	130	-35	-180	-180	180	-96	103
EPH 4000	173	41	-81	143	157	170	-71	-169	71	114	-178	-98	180	-178	180	-122	65
PTY 606	-104	-63	-56	170	83	175	-67	-177	63	95	-173	-162	156	-177	-175	-134	42
PTY 607	-108	-65	-72	171	81	-178	-60	-163	78	99	174	-171	151	-179	176	-103	-2
DGG 406(A)	132	—	—	—	—	17	141	171	49	57	170	146	-166	-122	-155	-91	-138
DGG 406(B)	-138	—	—	—	—	-49	180	-68	65	-95	-136	156	-158	-155	164	-106	-94

^a α_i , θ_i , β_i and γ_i are torsion angles of headgroup, glycerol backbone, *sn*-2 chain and *sn*-1 chain, respectively (see Fig. 2).

^b DMPC, dimyristoyl phosphatidylcholine crystal (Pascher et al. 1992); DLPE, dilauroyl phosphatidylethanolamine crystal (Pascher et al. 1992); PC2, distearoyl phosphatidylcholine with phosphatidylinositol transfer protein, PI-TP (PC2 501), bactericidal permeability-increasing protein, bpi (PC2 577 and 578); PLC, didodecanoyl phosphatidylcholine with *Thermomyces lanuginosa* lipase (PLC 601, 701, 801) and human pancreatic lipase-procolipase complex (PLC 1); DLP, dilinoleoyl phosphatidylcholine with phosphatidylcholine transfer protein, PC-TP; CPL, palmitoyl-linoleoyl phosphatidylcholine with PC-TP; LIO, pentadecanoyl-decanoyl phosphatidylcholine with *Acinetobacter calcoaceticus* ADP1 catechol-1,2-dioxygenase; PEH, distearoyl phosphatidylethanolamine with saposin B; EPH, phosphatidylethanolamine with *Helios virescens* ultraspiracle protein; PTY, pentadecanoyl-arachidoyl phosphatidylethanolamine with human recombinant soluble endothelial protein C receptor; DGG, palmitoyl-(*cis*-9,10-methylene)palmitoyl phosphatidyl(choline/glycerol) with *Alcaligenes eutrophus* flavohaemoprotein; where lipid identifiers are those from the PDB (see Table 1).

^c modeled; no electron density (Vetting and Ohlendorf 2000).

relatively infrequently in phospholipid crystals, all of which have a lamellar, membrane-like molecular arrangement (Pascher et al. 1992). In the latter case, *sc/sc* and *sc/-sc* configurations (as in DLPE and DMPC B, respectively), and to a lesser extent *-sc/-sc*, are strongly represented because of the intramolecular *gauche* effect. The *sc/ap* configuration occurs in one of the molecules (DMPC A) in crystals of dimyristoyl phosphatidylcholine (Pearson and Pascher 1979) and in dilauroyl phosphatidic acid (Pascher et al. 1992). For the former, the headgroup is directed away from the *sn*-2 chain, viz., the *sc/ γ /ap* configuration for which *sn*-1 is the leading chain, in the notation of Pascher et al. (1992). This is also the case for the phospholipids bound to PLA₂, thus exposing the ester group to hydrolytic attack (see Fig. 1C).

The *sc/-sc* configuration is found for phosphatidylethanolamine EPH 4000 bound to the *Helios virescens* ultraspiracle protein (USP), as well as for dilinoleoyl phosphatidylcholine DLP 2313 bound to the phosphatidylcholine transfer protein (PC-TP) and phosphatidylethanolamine PTY 606, 607 bound to the endothelial protein C receptor (rsEPCR). This configuration allows approximately parallel

alignment of the lipid chains and appears for one of the molecules (DMPC B) in crystals of dimyristoyl phosphatidylcholine, as the *sc/ γ /-sc* structure with leading *sn*-1 chain (Pearson and Pascher 1979). EPH 4000 bound to USP has a similar configuration, in which the headgroup is located over the lipid chains. DLP 2313 bound to the PC-TP more resembles the *sc/ β /-sc* structure with leading *sn*-2 chain and the headgroup directed away from the chains. For PTY bound to EPCR, the headgroup is directed away from the chains, which splay apart further down their length.

The *sc/sc* configuration, which also allows parallel alignment of the lipid chains, is reported for dilauroyl phosphatidylcholine PLC 701 and 801 bound to *Thermomyces lanuginosa* lipase. In the latter case, however, the lipid chains are not aligned parallel to one another but instead are oriented in opposite directions. This configuration, which is not found in the crystals of diacyl phospholipids, is achieved by means of an energetically forbidden *cis* conformation (γ_2) for the carboxyl ester group of the *sn*-1 chain (see Table 2).

The remainder of the phospholipid structures contain at least one eclipsed conformer in the glycerol backbone (or are the incorrect enantiomer). However, PLC 601 and INB

Table 3. Torsion angles ($^{\circ}$) of the inhibitory substrate analogs 1-octyl-2-heptylphosphonyl-sn-glycero-3-phosphoethanolamine (GEL), 1-octadecyl-2-acetamido-2-deoxy-sn-glycero-3-phosphoethyl methyl sulphide (INB), and 2-dodecanoyl-amino-1-hexanol-phosphoglycol (DHG), bound to various phospholipases A₂ (PLA₂) in crystals^a

Lipid ^b	PLA ₂ ^b	α_1	α_2	α_3	α_4	α_5	θ_1	θ_2	θ_3	θ_4	β_1	β_2	β_3	β_4	γ_1	γ_2	γ_3	γ_4	References
GEL930	cobra	101	86	95	108	154	53	174	-169	76	107	103	-16	165	102	-171	-131	117	White et al. 1990 (PDB:1POB)
GEL935		67	91	175	-121	114	51	-177	75	-54	129	117	-54	158	166	-13	148	91	White et al. 1990 (PDB:1POB)
GEL420	bee	91	94	-169	-123	133	61	-174	173	47	89	121	-161	161	109	-155	-131	-172	Scott et al. 1990 (PDB:1POC)
GEL930	synovial	96	83	68	169	-70	50	173	170	52	101	121	-40	173	103	169	160	-167	Scott et al. 1991 (PDB:1POE)
GEL935		95	81	85	177	-95	59	176	-170	76	106	114	-56	166	99	-170	-143	165	Scott et al. 1991 (PDB:1POE)
GEL150	pancreas	118	102	10	172	61	7	-179	-144	43	62	132	-21	172	108	-164	-59	-137	Sekar et al. 1998 (PDB:1MKV)
INB201	synovial	87	81	37	114	76	88	-148	-113	116	98	177			-85	170	172	-165	Oh 1995 (PDB:1AYP)
INB202		115	61	178	-113	170	86	-151	-151	85	119	178			84	157	152	172	Oh 1995 (PDB:1AYP)
INB203		128	64	166	125	-166	81	-153	-92	140	111	177			-107	-163	170	78	Oh 1995 (PDB:1AYP)
INB204		101	75	-175	-118	166	87	-151	-163	74	106	-176			140	-152	-175	164	Oh 1995 (PDB:1AYP)
INB205		113	63	72	148	-63	79	-158	-101	137	107	177			-100	-162	-173	173	Oh 1995 (PDB:1AYP)
INB206		81	79	57	115	70	71	-163	-162	71	110	178			138	164	162	-177	Oh 1995 (PDB:1AYP)
DHG126(A)	pancreas	92	70	74	136	74	85	-157	-157	83	117	180	-83	-50	82	-169			Thunnissen et al. 1990 (PDB:5P2P)
DHG126(B)		106	67	75	-173	-45	61	-169	-175	54	111	180	-85	-44	72	62			Thunnissen et al. 1990 (PDB:5P2P)

^a α_i , θ_i , β_i and γ_i are torsion angles of headgroup, glycerol backbone, *sn*-2 chain and *sn*-1 chain, respectively (see Fig. 2).

^b Cobra (*Naja naja*) venom PLA₂/GEL930,935 at 2.00 Å; honey bee venom PLA₂/GEL420 at 2.00 Å; human synovial fluid PLA₂/GEL930,935 at 2.10 Å; bovine pancreatic PLA₂/GEL150 at 1.89 Å; human synovial fluid PLA₂/INB 201-6 at 2.57 Å; pig pancreas PLA₂/DHG126(A),(B) at 2.40 Å, where lipid identifiers are those in the PDB.

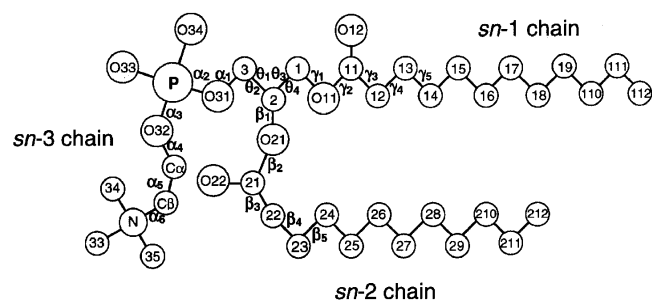


Figure 2. Designation of phospholipid torsion angles for the headgroup (α_i), glycerol backbone (θ_i), *sn*-1 chain (γ_i), and *sn*-2 chain (β_i). For the glycerol backbone: $\theta_1 \equiv$ C(1)-C(2)-C(3)-O(31), $\theta_2 \equiv$ O(21)-C(2)-C(3)-O(31), and $\theta_3 \equiv$ O(11)-C(1)-C(2)-C(3), $\theta_4 \equiv$ O(11)-C(1)-C(2)-O(21).

201 have values of θ_4/θ_2 that approximate to those of the other members of these two series. Palmitoyl-linoleoyl phosphatidylcholine, CPL 300 and 301, bound to the phosphatidylcholine transfer protein lie most closely to the *sc*/*-sc* staggered configuration, with the headgroup directed away from the chains (see Fig. 1B), as does DLP 2313 bound to PC-TP. The structure of phosphatidylethanolamine PEH 300 bound to saposin B approximates most nearly to a *sc*/*-sc* staggered configuration with parallel aligned chains and the headgroup directed away from the chains (see Fig. 1A).

The structures of phosphatidylcholine PLC1 bound to the pancreatic lipase–procolipase complex and of distearoyl phosphatidylcholine PC2 577 bound to the bactericidal permeability-inducing protein approximate to the *ap*/*sc* and *ap*/*-sc* staggered configurations in which the *sn*-1 and *sn*-2

Table 4. Glycerol backbone configuration of phospholipids in crystals of soluble proteins^a

Lipid ^b	Protein ^b	$\theta_1-\theta_2(^{\circ})$	$\theta_3-\theta_4(^{\circ})$	θ_4/θ_2	θ_3/θ_1
GEL 930,935	cobra PLA ₂	-126 ± 5	122 ± 7	sc,-sc/ap	(t,g ⁺)g ⁺
GEL 420	bee PLA ₂	-125	126	sc/ap	tg ⁺
GEL 930,935	synovial PLA ₂	-120 ± 3	116 ± 2	sc/ap	tg ⁺
GEL 150	pancreas PLA ₂	-173	173	sc/ap	s ⁻ c
INB 202,204,206	synovial PLA ₂	-124 ± 2	125 ± 1	sc/ap	tg ⁺
INB 203,205	synovial PLA ₂	-124 ± 1	125 ± 3	ac/ap	s ⁻ g ⁺
INB 201	synovial PLA ₂	-124	131	ac/-ac	s ⁻ g ⁺
DGH 126(A,B)	pancreas PLA ₂	-124 ± 6	125 ± 6	sc/ap	tg ⁺
PC2 501	rat PI-TP α	+108	-112	sc/ap	g ⁻ g ⁻
PC2 577	human bpip	-136	132	ac/-sc	g ⁻ s ⁺
PC2 578	human bpip	-	121	ac/-	s ⁻ -
PLC 601	<i>Th. lanuginosa</i> lipase	-133	131	sp/sc	ts ⁻
PLC 701,801	<i>Th. lanuginosa</i> lipase	-126	127 ± 1	sc/sc	tg ⁻
PLC 1	human pancreatic lipase	-130	130	ac/sc	g ⁻ g ⁻
DLP 2313	human PC-TP	-131	130	sc/-sc	ts ⁺
CPL 300,301	human PC-TP	-127 ± 1	126 ± 1	sc/-ac	ts ⁺
LIO 999,1999	Ac 1,2-CTD	-131	129	-ac/-ac	cs ⁺
PEH 300	human saposin B	-122	135	sp/-ac	ts ⁺
EPH 4000	<i>H. virescens</i> USP	-119	120	sc/-sc	tt
PTY 606,607	human rsEPCR	-118 ± 1	119	sc/-sc	tt
DGG 406(A)	<i>A. eutrophus</i> FHP	-125	132	sc/ac	tc
DGG 406(B)	<i>A. eutrophus</i> FHP	122	-133	sc/ap	g ⁻ g ⁻

^a Enantiomeric configuration is specified by the relative signs of θ_1 and θ_2 , or of θ_3 and θ_4 . θ_4/θ_2 gives the relative orientation of the *sn*-1 and *sn*-2 chains, and θ_3/θ_1 specifies the glycerol backbone conformation (see Pascher et al. 1992).

^b Nomenclature as defined in Tables 1 to 3.

chains are extended in opposite directions (see Fig. 1D). Such a configuration does not appear in known crystal structures of diacyl phospholipids, but is found as ap/-sc for the extended structure of crystalline *N*-dihydroxyoctadecanoyl-phytosphingosine (Pascher and Sundell 1992). It is most likely that phosphatidylcholines PLC 601, 701, and 801 bound to *Thermomyces lanuginosa* lipase that were discussed above also have one of these two configurations (with a *trans*, rather than *cis*, *sn*-1 chain carboxyl ester). In these configurations, the phosphatidylcholine headgroup is predominantly perpendicular to, and in the case of the lipases even encircled by, the lipid chains.

Headgroup conformation

The α_1 -torsion angle (C3-O) is mostly ap (*trans*) for the protein-bound phospholipids of Table 2, and ac (*skew*) for the PLA₂ inhibitors in Table 3 (as are also the non-*trans* conformers in Table 2). The *trans* rotamer is found in all crystals of phosphatidylethanolamine and its methylated derivatives, including phosphatidylcholine (Pascher et al. 1992). The *skew* rotamer is found in crystals of phosphatidylglycerol (see Pascher et al. 1987).

Correlated torsion angles $\alpha_2/\alpha_3 = \pm sc/\pm sc$ are expected on energetic grounds for the O-P-O sequence of phosphate

diesters (Gorenstein et al. 1976) and are found without exception in phospholipid crystals. Of the PLA₂ inhibitors in Table 3, approximately 60% have the sc/sc configuration for α_2/α_3 and approximately 40% have the energetically next most favorable sc/ap configuration. Of the protein-bound phospholipids in Table 2, only PTY 606, 607 has the $\alpha_2/\alpha_3 = \pm sc/\pm sc$ headgroup configuration and none has the $\pm sc/ap$ configuration. (The headgroup of LIO is not defined and only modeled in this region.)

In phospholipid crystals, the α_4 -torsion angle (O-C α) lies in the range from ap to $\pm ac$, which is also the case for all values of α_4 in Tables 2 and 3. The α_5 -torsion angle (C α -C β) is $\pm sc$ in crystals of phosphatidylethanolamine and all *N*-methylated derivatives, and ap in phosphatidylglycerol crystals. The $\alpha_5 = \pm sc$ conformation is favored by an internal electrostatic interaction between the phosphate and nitrogen charges, for example, for DMPC and DLPE. These values for α_5 are found for most of the protein-bound lipids in Table 3 and some of those in Table 2. An $\alpha_5 = ap$ rather than $\alpha_5 = \pm sc$ conformation can be favored for P-N headgroups by electrostatic interactions with the protein, and is found in several cases in Tables 2 and 3. Nonetheless, there are still an appreciable number of energetically disallowed eclipsed conformers for α_5 in the protein-bound phospholipids, especially those in Table 2. In total, 29% of the θ_1 , θ_2 , θ_3 , θ_4 , and α_5 torsion angles for the protein-bound lipids

in Tables 2 and 3 are in eclipsed conformations ($24\% \pm ac$ and $5\% sp$, compared with $31\% ap$ and $40\% \pm sc$).

Additional to bent-down conformations of the headgroup, which are those found in diacyl phospholipid crystals (Pascher et al. 1992) and in membranes (Seelig 1977), headgroups that are almost fully extended, or are strongly kinked or curled, are found for some protein-bound phospholipids. In the GEL inhibitor lipids bound to PLA₂, the headgroup is directed out from the lipid chains and the nitrogen away from the phosphate (see Fig. 1C). Multiple interactions with residues of the binding pocket are responsible for this headgroup orientation. The situation is similar for DHG bound to PLA₂, but less well defined—as regards distinct orientation—for the INB inhibitors.

For PLC 601, 701, and 801 phosphatidylcholine bound to *Th. lanuginosa* lipase, the headgroup is mostly *trans* (i.e., *ap*) in conformation and extends directly outwards from the glycerol backbone. A more curled configuration is found, however, for the headgroup of PLC 1 bound to the pancreatic lipase–procolipase complex (see Fig. 1D). For PC2 501 and PC2 577 bound respectively to the PI-transfer protein and the bactericidal permeability-increasing protein, the headgroup although not completely extended is also directed away from the chains. The phosphate group of PC2 is hydrogen bonded to, and interacts electrostatically with, neighboring side chains (Lys 195 and Thr 97 for PI-TP, and Tyr 455 for bpip); for PC2 501, the choline may also participate in electrostatic interaction (with Glu 86). The α -torsion angles of DLP 2313, and CPL 300 and 301, phosphatidylcholines bound to the PC-transfer protein, are essentially all *trans*, with the exception of α_3 , which is *cis*. This causes the headgroup to bend back over the chains (see Fig. 1B). The phosphate group of these lipids is hydrogen bonded to the protein (Tyr 72, Gln 157) and interacts with the neighboring arginine residue (Arg 78). The choline group participates in cation- π interactions with neighboring aromatic side chains (Trp 101, Tyr 114, and Tyr 155).

Phosphatidylethanolamine EPH 4000 bound to the ultraspiracle protein has a headgroup that is bent down towards the chains. This is caused by an H-bond interaction of the amine nitrogen with Gln 338 on the protein. For PEH 300 bound to saposin B, only the phosphate of the phosphatidylethanolamine headgroup interacts electrostatically and hydrogen bonds with the protein (with Arg 38), and the nitrogen is directed away from the chains (see Fig. 1A).

Chain configuration

For the diacyl phospholipids in Table 2, the torsion angles γ_2 and β_2 represent the carboxyl ester groups (O–CO) of the *sn*-1 and *sn*-2 chains, respectively. The conformation should therefore be *trans* (*ap*). However, only 56% of the γ_2 - and β_2 -torsion angles of the protein-bound phospholipids in Table 2 are *trans*; 25% are *cis*, and the remaining 19% are

nonplanar. In the case of PLC 601, 701, and 801, it was suggested above that this stereochemical violation could be the result of a misassignment of the backbone θ_4 -torsion angles.

Figure 3 shows the complete set of γ_n and β_n chain torsion angles (C_{n-2} – C_{n-1}) for the phospholipid ligands of selected proteins. The “allowed” ranges of *trans* (*ap*) and *gauche* ($\pm sc$) staggered rotamers are indicated by cross-hatching. It is seen that for each system not all torsion angles are in the allowed range. *Skew* ($\pm ac$) conformers, which appear in the $\pm 120^\circ$ nonhatched regions, are particularly prevalent, although they are only expected adjacent to double bonds because otherwise they are eclipsed. *cis* conformers (the 0° nonhatched regions) are expected only for double bonds (or cyclopropane rings), and they appear only at the expected positions C_9 – C_{10} ($n = 11$) and C_{12} – C_{13}

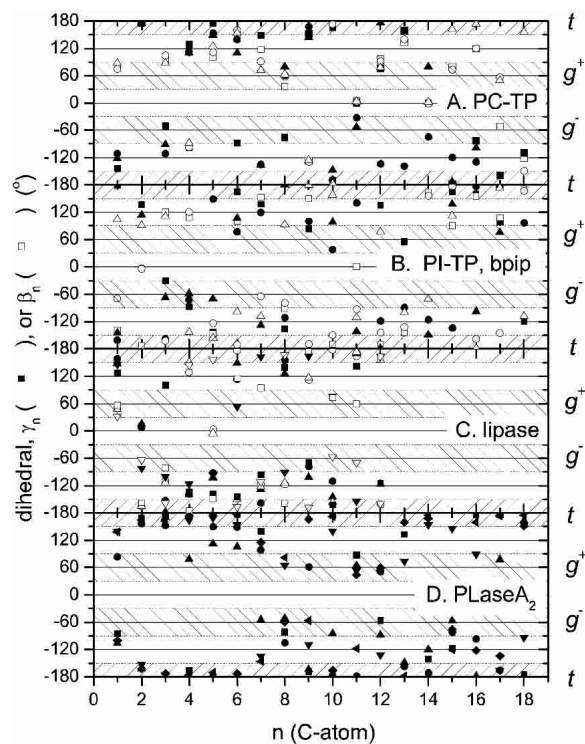


Figure 3. Torsion angles, $C_{n-3}C_{n-2}C_{n-1}C_n$, in the *sn*-1 (solid symbols) and the *sn*-2 (open symbols) chains of protein-bound phospholipids. A. Dilinoleoyl phosphatidylcholine (DLP; \blacksquare , \square) or 1-palmitoyl-2-linoleoyl phosphatidylcholine (CPL; \bullet , \circ ; \blacktriangle , \triangle) bound to the human phosphatidylcholine transfer protein (PDB: 1LN3, 1LN3; Roderick et al. 2002). B. Distearoyl phosphatidylcholine (PC2) bound to the α -isoform of rat phosphatidylinositol transfer protein (\blacksquare , \square) (PDB: 1FVZ; Yoder et al. 2001) or to the human bactericidal permeability-increasing protein (\bullet , \circ ; \blacktriangle , \triangle) (PDB: 1EWF; Kleiger et al. 2000). C. Dilauroyl phosphatidylcholine (PLC) bound to *Th. lanuginosa* lipase (\blacksquare , \square ; \bullet , \circ ; \blacktriangle , \triangle) (PDB: 1EIN; Brzozowski et al. 2000) or to human pancreatic lipase–procolipase complex (\blacktriangledown , \triangledown) (PDB: 1LPA; van Tilbeurgh et al. 1993). D. 1-*O*-octadecyl-2-acetamido-2-deoxy-*sn*-glycero-3-phosphoethyl methylsulphide (INB) bound to human synovial phospholipase A₂ (PDB: 1AYP; Oh 1995). Shapes of symbols are used to distinguish the individual lipids in each panel.

($n = 14$) for the linoleoyl chains associated with the PC-transfer protein (see Fig. 3A). A *cis* 9–10 bond is also found in the *sn*-1 and *sn*-2 chains of PC2 501 bound to the PI-transfer protein (Fig. 3B). This corresponds to the dioleoyl phosphatidylcholine used to displace bound bacterial phosphatidylglycerol, although it is named distearoyl phosphatidylcholine in the PDB. EPH 4000 bound to USP is designated as 1-palmitoyl-2-oleoyl phosphatidylethanolamine in the PDB. However, neither chain contains a *cis* bond, and the chainlengths correspond to 1-stearoyl-2-palmitoyl phosphatidylethanolamine, rather than to 1-palmitoyl-2-stearoyl phosphatidylethanolamine. A *cis* 9–10 conformation (β_{11}) is found for the cyclopropane ring in the *sn*-2 chain of DGG 406 bound to *A. eutrophus* FHP.

Table 5 lists the populations of chain rotamers for all the different lipids bound to the various proteins (see also Fig. 4). The *cis* conformers are mostly accounted for by double bonds or a cyclopropane ring. In many cases, however, energetically disallowed eclipsed *skew* conformations predominate to a far greater extent than would be allowed for by the double-bond, or cyclopropane, content. For phosphatidylethanolamine PEH 300 bound to saposin, this difficulty almost certainly results from the reported conformational heterogeneity. For the other similar situations, the eclipsed conformations probably also represent a superposition of allowed rotamers, rather than a single unique configuration with exceptionally high conformational energy (~ 3 kcal/mole per *skew* conformation). Only 39% of the C–C bonds in Table 5 are in the *trans* (ap) conformation. This compares with approximately 70% *trans* bonds for the lipid chains in fluid bilayer membranes (see, e.g., Cevc and Marsh 1987; Moser et al. 1989). Summing all torsion angles $>120^\circ$ and $<-120^\circ$ in Figure 4 still yields an effective total *trans* population of only 62%. The postulated conformational heterogeneity makes precise comparisons difficult, but it appears that the chains of the phospholipid ligands are conformationally more disordered in the protein binding pockets than they are in fluid lipid membranes.

Table 5. Distribution (%) of acyl chain torsion angles for phospholipids in crystals of soluble proteins

lipid ^a	<i>trans</i> (ap)	eclipsed ($\pm ac$)	<i>gauche</i> ($\pm sc$)	<i>cis</i> (sp)	N^b
GEL	42	47	8	3	60
PC2	31	51	16	2	90
PLC	37	49	11	3	72
DLP	27	37	23	13	30
CPL	25	43	25	7	56
LIO	55	42	3	0	38
PEH	48	41	11	0	27
EPH	32	39	29	0	28
PTY	43	33	21	3	58
DGG	50	23	23	4	52

^a Nomenclature as in Tables 1 to 3, which list the proteins involved.

^b Total number of torsion angles, β_n and γ_n with $n > 3$.

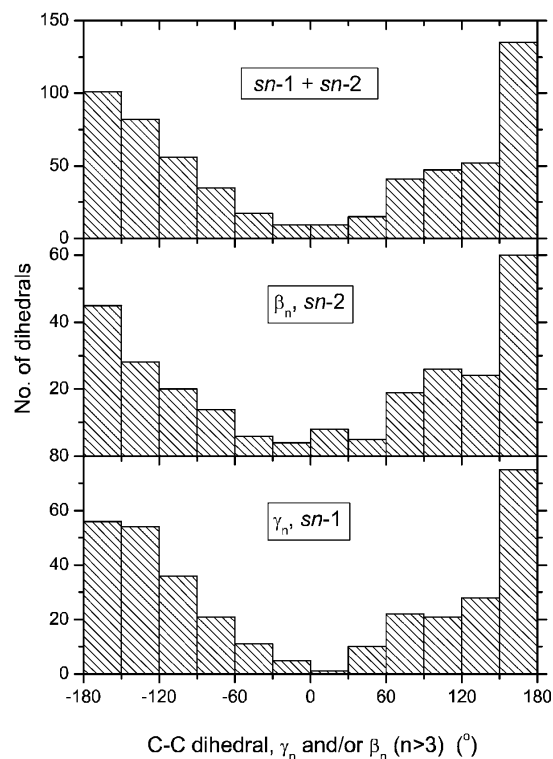


Figure 4. Distribution of torsion angles, γ_n and β_n ($n > 3$), in the hydrocarbon chains of the protein-bound phospholipids listed in Tables 1 to 3 (with the exception of DHG). From upper to lower: all chains ($N = 599$); all *sn*-2 chains ($N = 259$); all *sn*-1 chains ($N = 340$).

Conclusions

The phospholipid ligands of lipid-binding proteins display a considerably greater range of conformations than do phospholipids in crystals. Several of these configurations (e.g., for the lipases and phospholipid transfer proteins) are not compatible with those in the donor or acceptor membranes with which they interact. Configurations are found with oppositely directed lipid chains, rather than the parallel chain stacking required in membranes. Extended lipid headgroups, and other headgroup orientations that are directed away from the lipid chains, appear to optimize polar interactions with residues within the lipid binding pocket, in many cases. These situations are quite different from the bent-down headgroup configuration found in phospholipid crystals and biological membranes. The lipid chains are conformationally disordered within the protein binding site, probably to a greater extent than the dynamic disorder in fluid membranes. Not all of the phospholipid ligand structures in the PDB are stereochemically acceptable, in the sense of incorrect glycerol enantiomer and either nonplanar or *cis* carboxyl ester conformations. Furthermore, the preponderance of eclipsed C–C bond conformers in the lipid chains strongly suggests the possibility of conformational heterogeneity of the bound lipids. It is, of course, possible

that the occurrence of eclipsed conformers also reflects limitations in the accuracy of the crystal structures. However, the former bears no obvious relation to the resolution of the structure determinations (cf. Table 1 and Fig. 3) and—as already mentioned—there is evidence for conformational heterogeneity from the electron density maps, in at least one case (Ahn et al. 2003).

Acknowledgments

The publication costs of this article were defrayed in part by payment of page charges. This article must therefore be hereby marked “advertisement” in accordance with 18 USC section 1734 solely to indicate this fact.

References

- Ahn, V.E., Faull, K.F., Whitelegge, J.P., Fluharty, A.L., and Prive, G.G. 2003. Crystal structure of saposin B reveals a dimeric shell for lipid binding. *Proc. Natl. Acad. Sci.* **100**: 38–43.
- Billas, I.M.L., Moulinier, L., Rochel, N., and Moras, D. 2001. Crystal structure of the ligand-binding domain of the ultraspiracle protein USP, the ortholog of retinoid X receptors in insects. *J. Biol. Chem.* **276**: 7465–7474.
- Brzozowski, A.M., Savage, H., Verma, C.S., Turkenburg, J.P., Lawson, D.M., Svendsen, A., and Patkar, S. 2000. Structural origins of the interfacial activation in *Thermomyces (Humicola) lanuginosa* lipase. *Biochemistry* **39**: 15071–15082.
- Cevc, G. and Marsh, D. 1987. *Phospholipid bilayers. Physical principles and models*. Wiley-Interscience, New York.
- Elder, M., Hitchcock, M.P., Mason, R., and Shipley, G.G. 1977. A refinement analysis of the crystallography of the phospholipid, 1,2-dilauroyl-DL-phosphatidylethanolamine, and some remarks on lipid–lipid and lipid–protein interactions. *Proc. R. Soc. Lond. A* **354**: 157–170.
- Gorenstein, D.G., Kar, D., Luxon, B.A., and Momii, R.K. 1976. Conformational study of cyclic and acyclic phosphate esters. CNDO/2 calculations of angle strain and torsional strain. *J. Am. Chem. Soc.* **98**: 1668–1673.
- Hurley, J.H., Tsujishita, Y., and Pearson, M.A. 2000. Floundering about at cell membranes: A structural view of phospholipid signaling. *Curr. Opin. Struct. Biol.* **10**: 737–743.
- Kleiger, G., Beamer, L.J., Grothe, R., Mallick, P., and Eisenberg, D. 2000. The 1.7 Å crystal structure of BPI: A study of how two dissimilar amino acid sequences can adopt the same fold. *J. Mol. Biol.* **299**: 1019–1034.
- Moser, M., Marsh, D., Meier, P., Wassmer, K.-H., and Kothe, G. 1989. Chain configuration and flexibility gradient in phospholipid membranes. Comparison between spin-label electron spin resonance and deuterium nuclear magnetic resonance, and identification of new conformations. *Biophys. J.* **55**: 111–123.
- Oganesyan, V., Oganesyan, N., Terzyan, S., Qu, D.F., Dauter, Z., Esmon, N.L., and Esmon, C.T. 2002. The crystal structure of the endothelial protein C receptor and a bound phospholipid. *J. Biol. Chem.* **277**: 24851–24854.
- Oh, B.-H. 1995. A probe molecule composed of seventeen percent of total diffracting matter gives correct solutions in molecular replacement. *Acta Crystallogr. D* **51**: 140–144.
- Ollesch, G., Kaunzinger, A., Juchelka, D., Schuber-Zsilavec, M., and Ermler, U. 1999. Phospholipid bound to the flavohemoprotein from *Alcaligenes eutrophus*. *Eur. J. Biochem.* **262**: 396–405.
- Pascher, I. and Sundell, S. 1992. Molecular arrangements in sphingolipids—Crystal structure of the ceramide *N*-(2D,3D-dihydroxyoctadecanoyl)-phosphatidylcholine. *Chem. Phys. Lipids* **62**: 79–86.
- Pascher, I., Sundell, S., Harlos, K., and Eibl, H. 1987. Conformation and packing properties of membrane lipids: The crystal structure of sodium dimyristoylphosphatidylglycerol. *Biochim. Biophys. Acta* **896**: 77–88.
- Pascher, I., Lundmark, M., Nyholm, P.-G., and Sundell, S. 1992. Crystal structures of membrane lipids. *Biochim. Biophys. Acta* **1113**: 339–373.
- Pearson, R.H. and Pascher, I. 1979. The molecular structure of lecithin dihydrate. *Nature* **281**: 499–501.
- Roderick, S.L., Chan, W.W., Agate, D.S., Olsen, L.R., Vetting, M.W., Rajashankar, K.R., and Cohen, D.E. 2002. Structure of human phosphatidylcholine transfer protein in complex with its ligand. *Nat. Struct. Biol.* **9**: 507–511.
- Scott, D.L. and Sigler, P.B. 1994. Structure and catalytic mechanism of secretory phospholipase A₂. *Adv. Protein Chem.* **45**: 53–88.
- Scott, D.L., Otwinowski, Z., Gelb, M.H., and Sigler, P.B. 1990. Crystal structure of bee-venom phospholipase A₂ in a complex with a transition-state analogue. *Science* **250**: 1563–1566.
- Scott, D.L., White, S.P., Browning, J.L., Rosa, J.J., Gelb, M.H., and Sigler, P.B. 1991. Structures of free and inhibited human secretory phospholipase A₂ from inflammatory exudate. *Science* **254**: 1007–1010.
- Seelig, J. 1977. Deuterium magnetic resonance: Theory and application to lipid membranes. *Q. Rev. Biophys.* **10**: 358–418.
- Sekar, K., Kumar, A., Liu, X., Tsai, M.D., Gelb, M.H., and Sundaralingam, M. 1998. Structure of the complex of bovine pancreatic phospholipase A₂ with a transition-state analogue. *Acta Crystallogr D* **54**: 334–341.
- Thunnissen, M.M.G.M., Eiso, A.B., Kalk, K.H., Drenth, J., Dijkstra, B.W., Kuipers, O.P., Dijkman, R., de Haas, G.H., and Verheij, H.M. 1990. X-ray structure of phospholipase A₂ complexed with a substrate derived inhibitor. *Nature* **347**: 689–691.
- van Tilbeurgh, H., Egloff, M.P., Martinez, C., Rugani, N., Verger, R., and Cambillau, C. 1993. Interfacial activation of the lipase-procolipase complex by mixed micelles revealed by X-ray crystallography. *Nature* **362**: 814–820.
- Vetting, M.W. and Ohlendorf, D.H. 2000. The 1.8 Å crystal structure of catechol 1,2-dioxygenase reveals a novel hydrophobic helical zipper as a subunit linker. *Struct. Fold. Des.* **8**: 429–440.
- Wallace, A.C., Laskowski, R.A., and Thornton, J.M. 1995. LIGPLOT—A program to generate schematic diagrams of protein ligand interactions. *Protein Eng.* **8**: 127–134.
- White, S.P., Scott, D.L., Otwinowski, Z., Gelb, M.H., and Sigler, P.B. 1990. Crystal structure of cobra-venom phospholipase A₂ in a complex with a transition-state analogue. *Science* **250**: 1560–1563.
- Yoder, M.D., Thomas, L.M., Tremblay, J.M., Oliver, R.L., Yarbrough, L.R., and Helmkamp Jr., G.M. 2001. Structure of a multifunctional protein. *J. Biol. Chem.* **276**: 9246–9252.